

Elastic Anisotropy of Shales ... Revisited*

Marina Pervukhina¹ and Patrick N. J. Rasolofosaon²

Search and Discovery Article #41557 (2015)**

Posted February 16, 2015

*Adapted from article published in AAPG European Region Newsletter, June, 2014. Appreciation is expressed to AAPG European Region Council, Keith Gerdes, President, their Editorial Board, Viki Wood, Chief Editor, William Sassi, Coordinator R&D Projects, and Jeremy Richardson, Office Director, AAPG European Region.

**AAPG European Regional Newsletter©2014. Serial rights given by author. For all other rights contact author directly.

¹CSIRO, Earth Science and Resource Engineering, Australia (Marina.Pervukhina@csiro.au)

²IFP Énergie nouvelles, Rueil-Malmaison, France

Introduction

The presence of fractures and/or shale are among the main causes of seismic anisotropy in geological media, as is the case for instance in the recently discovered offshore pre-salt oil reservoirs of Brazil. Seismic anisotropy induced by the presence of shale is the topic of this study. By combining two shale databases (Thomsen, 1986; Pervukhina et al., 2013), we aim to extract the major trends in the relation between seismic anisotropy and compaction/diagenesis. More precisely the main objective of our work is to check if there is any major link between shale anisotropy and compaction.

The Considered Experimental Databases on Shale

Two anisotropy databases are considered in this work. The first database (Thomsen, 1986) appeared to be a nearly exhaustive database at the time of its publication (Thomsen, personal communication). It is composed of 59 samples of shales or shaly formations. The second database (Pervukhina et al., 2013) is composed of 37 shale samples with different mineralogical compositions, silt, and clay fractions, and porosities. Both databases are combined in order to analyze the major trends with respect to seismic anisotropy and compaction. Note that this composite shale database is characterized by its great diversity, either in terms of mineral composition, or in terms of burial depth and geologic age, and as a consequence in terms of level of compaction/diagenesis.

Definition of the Considered Anisotropic Parameters

All the considered rock samples are assumed transversely isotropic (TI) with a vertical symmetry axis. The anisotropy parameters considered in the present work are the classical parameters ϵ , δ , γ , and σ first introduced by Thomsen (1986), and illustrated by [Figure 1](#).

The first anisotropy parameter ε is roughly the relative difference between the P-wave velocities in the horizontal direction and in the vertical direction. The anisotropy parameter γ is the equivalent of the parameter ε for the SH-wave (i.e., the horizontally polarized S-wave). The parameter γ happens to be also equal to the S-wave birefringence coefficient for propagation in the horizontal direction. More precisely, γ is also roughly equal to the relative difference between the SH-wave velocity and the SV-wave (i.e., the vertically polarized S-wave) velocity for propagation in the horizontal direction.

The third parameter δ , that is to say the P-wave moveout parameter, is roughly equal to the relative difference between the P-wave moveout velocity and the P-wave vertical velocity. The last parameter σ , that is to say the SV-wave moveout parameter, is the equivalent of the parameter δ for the SV-wave. Note that the SH-wave moveout parameter is also equal to γ .

Effect of Burial and Compaction on Sediment Properties

One of the most important effect of burial on sedimentary formations is the reduction of porosity and the velocity and stiffening increase (e.g., Nafe et al., 1960; Gardner et al., 1974). In seismics, many empirical relationships between porosity, or velocity, and the depth of burial and geologic age are used (e.g., Bourbié et al., 1987; Mavko et al., 1998). Shale, as any sedimentary formation, is not an exception to the rule. A practical consequence is the trend observed on the shale database, and illustrated by [Figure 2](#), corroborating the simultaneous increase of both P-wave vertical velocity V_p , and S-wave vertical velocity V_s , with the density ρ . The corresponding depth data being available for only some of the considered samples actually corroborate the effect of burial both on densities and on velocities.

Effect on the Anisotropy Parameters

Up to now we did not deal with anisotropy. Here we check if the anisotropy parameters of shale follow some general trend linked with compaction. For this, crossplots similar to those of the previous figure are shown on [Figure 3](#) between the anisotropy parameters ε (blue diamonds), δ (red squares), γ (yellow triangles) and σ (green circles) and the qP-wave vertical velocity V_p (left), or the qS-wave vertical velocity (right). In contrast with the previous figures, no clear trend is observed for any of the anisotropy parameters. The systematic absence of anisotropy increase with velocity increase seems to imply that burial and/or compaction has no first order effect on seismic anisotropy increase. In other words, contrary to what has been conjectured by some authors (e.g., Hornby, 1995), there is no first order correlation between compaction and anisotropy strength. This is one of the main results of the present work.

Furthermore, there even seems to be a weak reversal trend between the anisotropy parameters ε (blue diamonds) and σ (green circles), and both velocities. This very rough decrease of ε and σ with velocity increase can simply be explained by the increase of both velocities V_p and V_s with compaction/diagenesis. Because both velocities are present in the denominators of the mathematical expressions of the anisotropy parameters (details to follow), an increase of both reference velocities V_p and V_s tends to slightly decrease any of the anisotropy parameters. Another possible explanation of the anisotropy decrease with the velocity increase is that the latter is caused with the increase of silt fraction, the fraction of nonclay minerals. Typically the increase of the silt fraction results in lower anisotropy parameters (Pervukhina et al., 2007). However, this effect is small if silt inclusions are distributed as isolated inclusions floating in the clay matrix.

Relation between the Anisotropy Parameters

In contrast, the crossplot between the anisotropy parameters γ and ε exhibits clear positive correlation, as illustrated by [Figure 4](#). In other words one observes an increase of γ with ε . Note that this is not the case for the remaining anisotropy parameters δ and σ (not shown here for conciseness). This is in agreement with the theoretical work of Sayers (2005), who described the elastic anisotropy of shales, assuming transverse isotropy for both the “crystal” symmetry and the Orientation Distribution Function of the “crystals.” We put the word crystal between quotation marks because, instead of crystals, shale is arranged in groups of parallel clay platelets, called “domains” by Aylmore and Quirk (1959). The main result, that the more aligned are the clay platelets, the larger the anisotropy parameters γ and ε , is corroborated by many experimental results. Note that this is not so clear for the remaining anisotropy parameters. Thus the increase of γ with ε observed in [Figure 4](#) is not really surprising and is linked with the orientation of the clay platelets. Furthermore, because neither γ nor ε increases with any of the velocities V_p and V_s , the increase of the clay platelets alignment is definitely not linked to the level of compaction, at least to the first order, as sometimes conjectured.

Discussion

First of all we are aware that the intrinsic anisotropy of the clay platelets and their orientation distribution function are not the only causes of elastic anisotropy in shale. Some complicating factors, such as the anisotropic distributions of discontinuities/porosity and the presence of aligned silt inclusions have drawn much less attention but have also been studied (e.g., Pervukhina et al., 2007; Pervukhina et al., 2013; Tiwary, 2007). However, because the shale samples of Pervukhina et al. (2013) have been included in our database, we think that these complicating factors should not substantially change the above conclusions, at least to the first order. Furthermore, note that the actual existence of such discontinuities in shale in natural conditions is still controversial (e.g., Zinszner et al., 2002; Rasolofosaon and Zinszner, 2014).

Because compaction can be excluded as a major cause of seismic anisotropy in shale, shale platelet alignment, clearly concomitant with the presence of seismic anisotropy in shale, can simply be due, for instance, to the conditions of deposition of the sediments. For instance, in turbiditic environment one would expect a stochastic misalignment of the clay platelets, inducing quasi-random Orientation Distribution Function of the clay platelets. As a consequence we could expect weak overall seismic anisotropy. In contrast, in a quiet depositional environment, one would expect a good alignment of the clay platelets in the direction perpendicular to the gravity at the time of sediment deposition. As a consequence the resulting seismic anisotropy is expected to be stronger.

Conclusions

By combining the two shale databases (Thomsen, 1986; Pervukhina et al., 2013) we extracted the major trends in the relation between seismic anisotropy and compaction. It clearly appears that compaction does not play a first order role in seismic anisotropy. As a consequence the increase of the clay platelets alignment is definitely not linked to the level of compaction, at least to the first order, as sometimes conjectured.

Otherwise there would be a systematic correlation between the increase of anisotropy strength and the velocity increase, which is at odds of what is experimentally observed. Furthermore, compaction/diagenesis tending to increase all the velocities, in particular the reference vertical P and S-wave velocities in the definition of the anisotropy parameters, even somehow contributes to weakly decrease the anisotropy parameters, which is roughly observed experimentally. In spite of some first attempts (Pervukhina et al., 2013). Rock Physics models that completely describe these major trends are still lacking and are strongly encouraged.

Acknowledgements

M. Pervukhina is grateful to CSIRO internally funded Multiphysics Rock Characterization project for support. P. Rasolofosaon gratefully acknowledges IFP Energies Nouvelles for permission to present this contribution.

References Cited

Aylmore, L.A.G., and J.P. Quirk, 1959, Swelling of clay-water system: *Nature*, v. 183, p. 1752-1753.

Bourbié, T., O. Coussy, and B. Zinszner, 1987, *Acoustics of Porous Media*: Editions Technip, Paris.

Gardner, G.H.F., L.W. Gardner, and A.R. Gregory, 1974, Formation velocity and density—The diagnostic basics for stratigraphic traps: *Geophysics*, v. 39, p. 770-780.

Hornby, B.E., 1995, *The elastic properties of shales*: Ph.D. dissertation, Cambridge University, Cambridge, England, 201 p.

Mavko, G., T. Mukerji, and J. Dvorkin, 1998, *The Rock Physics Handbook*: Cambridge University Press, 329 p.

Nafe, J.E., and C.L. Drake, 1960, Physical properties of marine sediments, *in* M.N. Hill, editor, *The Sea*, v. 3: Interscience, New-York, p. 794–815.

Pervukhina, M., A.F. Siggins, D.N. Dewhurst, and B. Gurevich (2007), Elastic properties of shales with respect to silt fraction, in ASEG, Perth, Australia.

Pervukhina, M., P. Golodoniuc, and D.N. Dewhurst, 2013, Phenomenologic study of seismic anisotropy in shales: 75th EAGE Conference & Exhibition incorporating SPE EUROPEC 2013 London, UK, paper We-P15-05.

Rasolofosaon, P.N.J., and B.E. Zinszner, 2014, *Petroacoustics – A tool for applied seismics*: EDP Sciences, website accessed January 31, 2015 (<http://books.ifpenouvelles.fr/ebooks/home/index.htm>).

Sayers, C.M., 2005, Seismic anisotropy of shales: *Geophysical Prospecting*, v. 53, p. 667–676.

Thomsen, L., 1986, Weak elastic anisotropy: *Geophysics*, v. 51, p. 1954–1966.

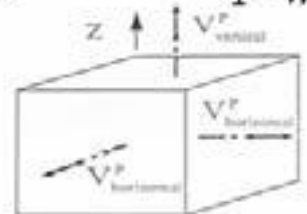
Tiwary, D.K., 2007, Mathematical modeling and ultrasonic measurement of shale anisotropy and a comparison of upscaling methods from sonic to seismic: Ph.D. dissertation, University of Oklahoma.

Zinszner, B., P. Meynier, J. Cabrera, and P. Volant, 2002, Vitesse des ondes ultrasonores, soniques et sismiques dans les argilites du tunnel de Tournemire: *Oil & Gas Science and Technology – Rev. IFP*, v. 57/4, p. 341-353.

$$V_{\text{vertical}}^P \quad \text{P-wave vertical velocity}$$

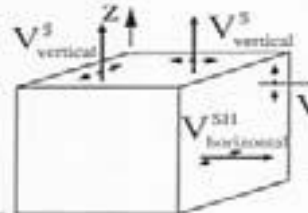
$$V_{\text{vertical}}^S \quad \text{S-wave vertical velocity}$$

ϵ P-wave "anisotropy"



$$\epsilon = \frac{(V_{\text{horizontal}}^P)^2 - (V_{\text{vertical}}^P)^2}{2(V_{\text{vertical}}^P)^2}$$

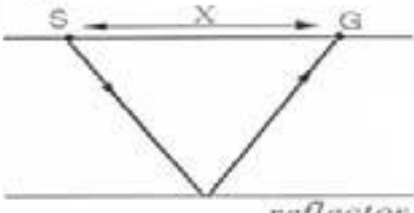
γ SH-wave "anisotropy" and S-wave birefringence



$$\gamma = \frac{(V_{\text{horizontal}}^{\text{SH}})^2 - (V_{\text{vertical}}^{\text{SH}})^2}{2(V_{\text{vertical}}^{\text{SH}})^2}$$

$$\gamma = \frac{(V_{\text{horizontal}}^{\text{SH}})^2 - (V_{\text{horizontal}}^{\text{SV}})^2}{2(V_{\text{horizontal}}^{\text{SV}})^2}$$

δ P-wave moveout parameter



$$\delta = \frac{(V_{\text{NMO}}^P)^2 - (V_{\text{vertical}}^P)^2}{2(V_{\text{vertical}}^P)^2}$$

t : traveltime
x : offset

Normal MoveOut
NMO velocity

$$\frac{1}{V_{\text{NMO}}^2} = \lim_{X \rightarrow 0} \frac{d(t^2)}{d(X^2)}$$

γ SH-wave moveout parameter
 σ SV-wave moveout parameter

$$\sigma = \left(\frac{V_{\text{vertical}}^P}{V_{\text{vertical}}^S} \right)^2 (\epsilon - \delta)$$

$$\epsilon = \frac{C_{11} - C_{33}}{2C_{33}}$$

$$\delta = \frac{(C_{13} + C_{44})^2 - (C_{33} - C_{44})^2}{2C_{33}(C_{33} - C_{44})}$$

$$\gamma = \frac{C_{66} - C_{44}}{2C_{44}}$$

Figure 1. Definitions of the anisotropy parameters ϵ , δ , γ , and σ of VTI and their link with measurable quantities for the P wave (left) and for the S waves (right).

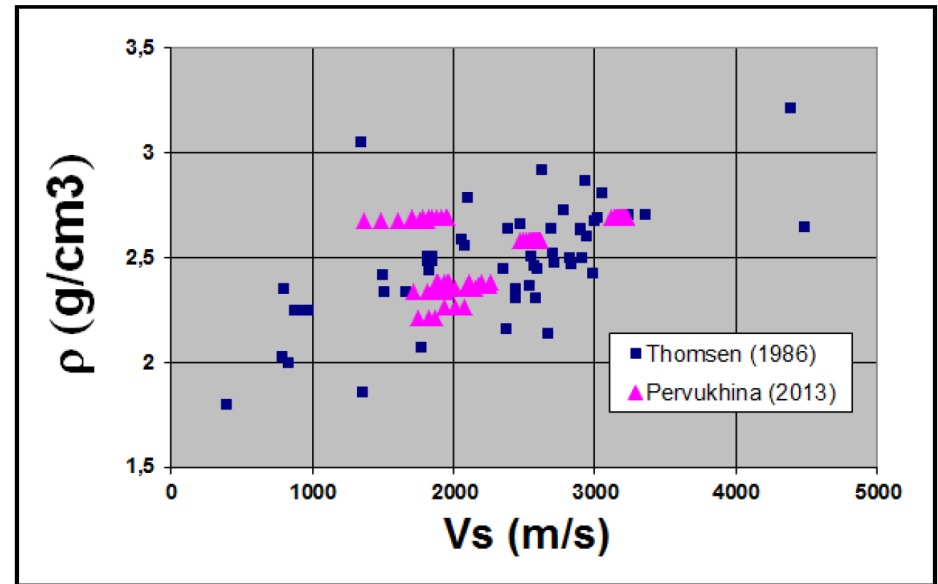
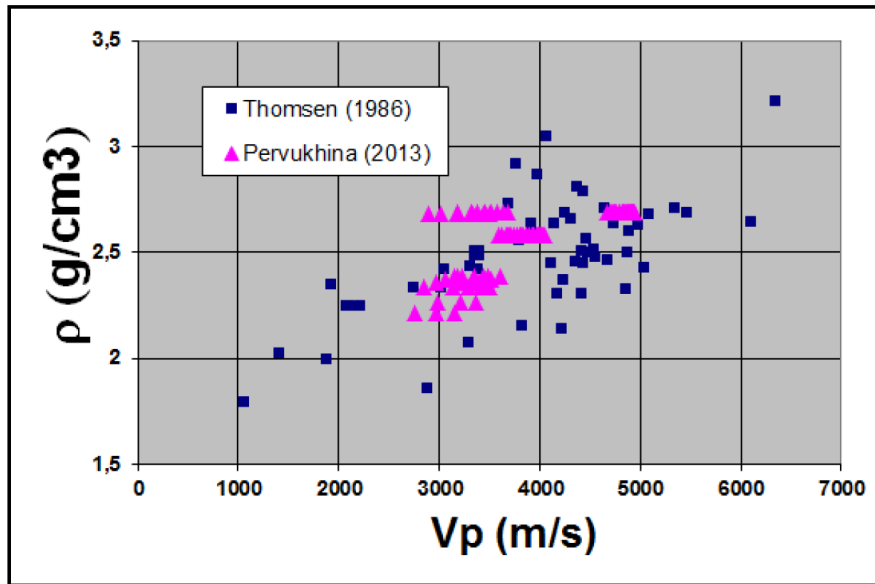


Figure 2. Left: Density ρ as function of the P-wave vertical velocity V_p . Right: Density ρ as function of the S-wave vertical velocity V_s . Both from the shale database of Thomsen (1986) and Pervukhina et al. (2013).

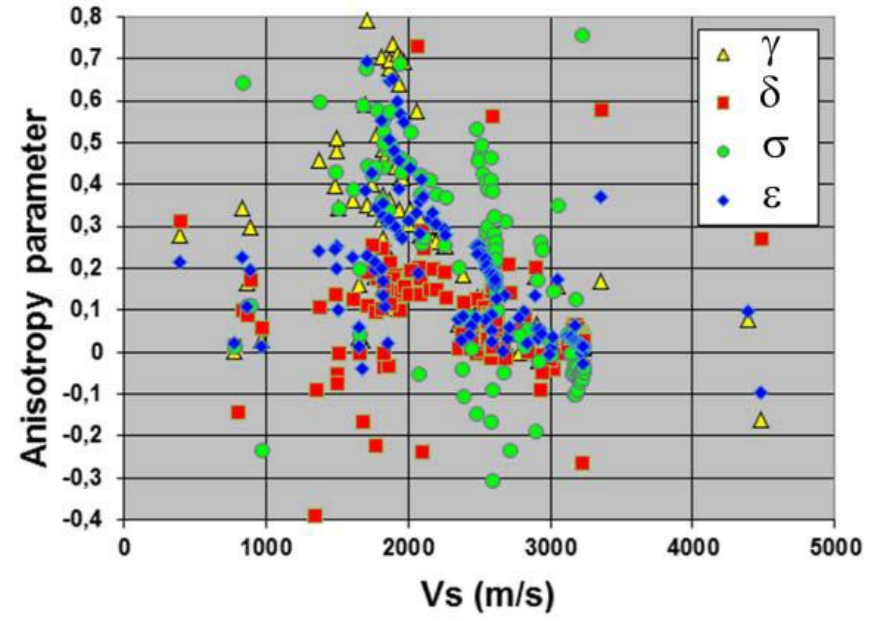
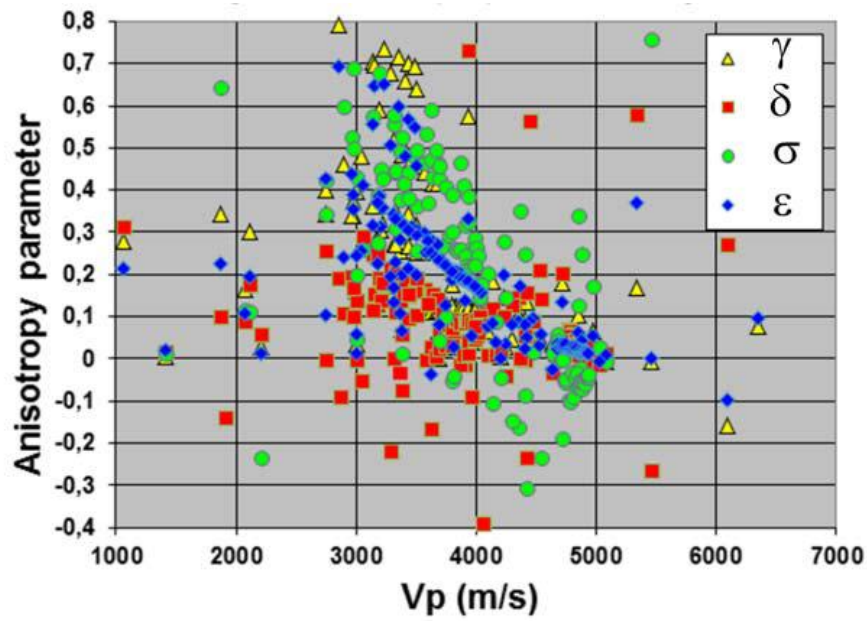


Figure 3. Left: Crossplot between the anisotropy parameters ϵ , δ , γ , and σ and the qP-wave vertical velocity V_p . Right: Crossplot between the anisotropy parameters ϵ , δ , γ , and σ and the qS-wave vertical velocity V_s .

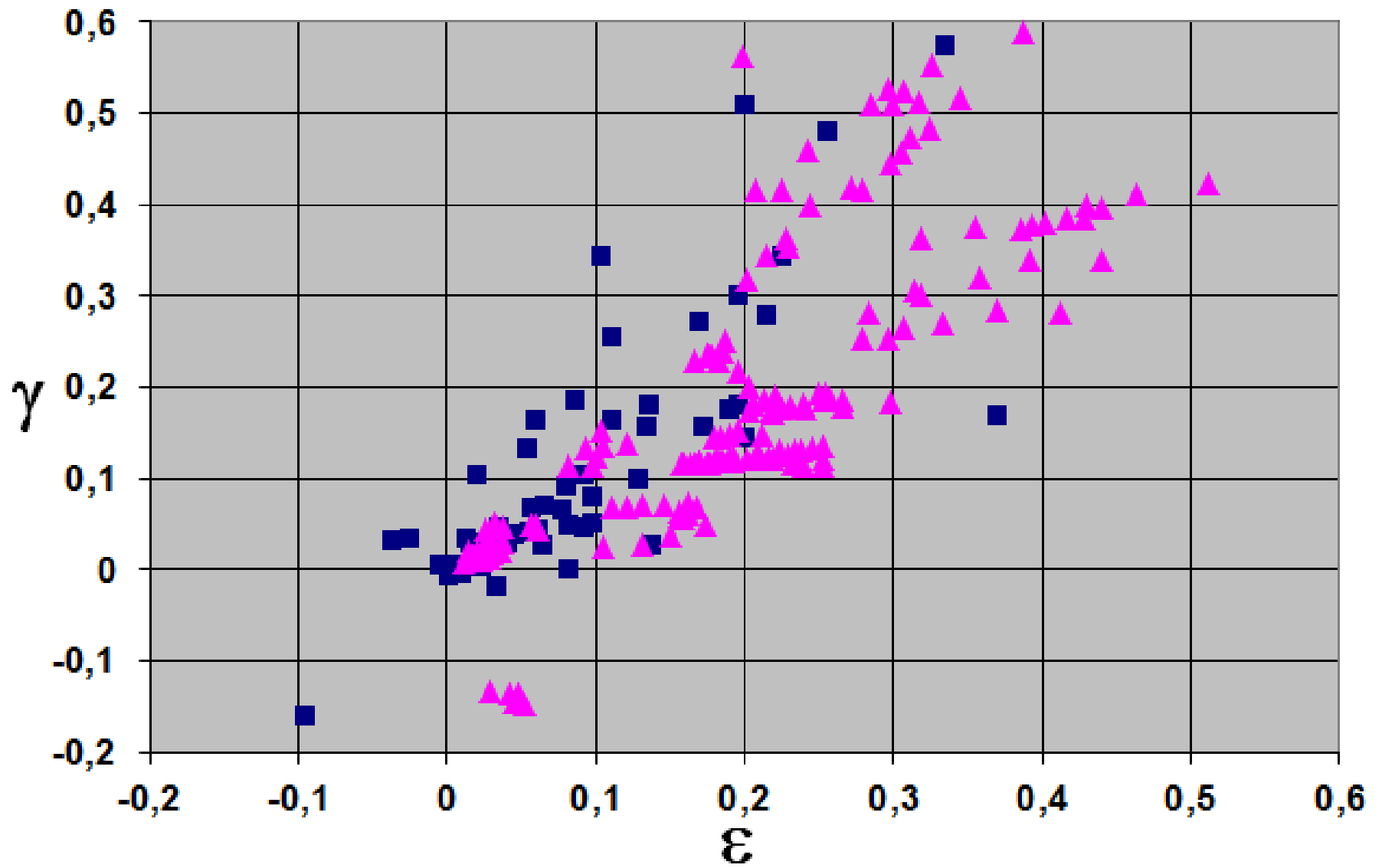


Figure 4. Crossplot of the anisotropy parameters ε and γ from the shale database of Thomsen (1986) and Pervukhina et al. (2013).